Peer-reviewed version available at *Energies* **2020**, *13*, 591; doi:10.3390/en13030591

*Article*

# Surface Discharges and Flashover Modelling of Solid Insulators in Gases

**Mohammed El Amine Slama [1], Abderrahmane Beroual [2] and Abderrahmane (Manu) Haddad [3]**

[1*] Advanced High Voltage Engineering Centre. School of Engineering. Cardiff University. Queen's Buildings The Parade, Cardiff CF24 3AA, Wales, United Kingdom. Email: slamame@cardiff.ac.uk

[2] Laboratoire Ampère. University of Lyon. 36 Avenue Guy de Collongues, Ecully, France. Email: abderrahmane.beroual@ec-lyon.fr

[3] Advanced High Voltage Engineering Centre. School of Engineering. Cardiff University. Queen's Buildings The Parade, Cardiff CF24 3AA, Wales, United Kingdom. Email: haddad@cardiff.ac.uk

**Abstract:** The aim of this paper is the presentation of an analytical model of insulator flashover and its application for air at atmospheric pressure and pressurized $SF_6$. After a review of the main existing models in air and compressed gases, we develop a relationship of flashover voltage on the basis of an electrical equivalent circuit and the thermal properties of the discharge. The model includes the discharge resistance, the insulator impedance and the gas interface impedance. The application of this model to a cylindrical resin-epoxy insulators in air medium and $SF_6$ gas with different pressures gives results close to the experimental measurements.

**Keywords:** surface discharge; flashover; gas; modelling; pressure; thermal properties

## 1. Introduction

In order to optimize the insulation level for high voltage components (Air Insulated Substations -AIS-, Gas Insulated Substations -GIS- and Gas Insulated Lines-GIL-, Breakers, Overhead lines…), a special attention is given to creeping or surface discharges because the thermal effects and the faults that they can produce by sparking or flashover. Then, the knowledge of the parameters characterizing this kind of discharge is essential to understand the complexity of the mechanisms involving in their development. Thus, it is fundamental to acquire such information enabling to build mathematical model that can help optimizing the insulation efficiency.

This paper aims to carry out a review of existing models of creeping discharges and to propose an analytical approach for the calculation of flashover voltage of solid insulators in gases under lightning voltage stress.

## 2. Review of surface discharges and flashover models in gases

From the insulation viewpoint, the triple junction (metal-gas-solid) constitutes the weakest point in high voltage equipment. Indeed, when the electric field reaches a critical value, partial discharges (PDs) can be initiated in the vicinity of this region. The increase of the voltage leads these PDs to develop and to transform into surface discharges (creeping discharges) that propagate over the

Peer-reviewed version available at Energies 2020, 13, 591; doi:10.3390/en13030591



insulator up to flashover [1 - 3]. In the case of GIS and GIL, the worst case is when insulators (spacer, post-type insulator) are contaminated by metallic particles on their surfaces [5, 6].

The physical mechanisms responsible for the surface discharge propagation are not still well known because of the complexity of the phenomena and the interaction of different factors, such as the interaction between the discharges, nature of gas and the proprieties of the solid insulating material, gas pressure, surface charges and pollution (metallic particle), geometrical parameters (insulator shape, electrodes form…), etc. Fundamentals studies have been conducted to understand the inception and propagation of creeping discharges in various gases [7 - 14]. It appears from the reported results that the phenomena start with corona discharges that evolves into ramified streamers. When the streamer discharge reaches a certain length, a leader channel with streamers at its head appears.

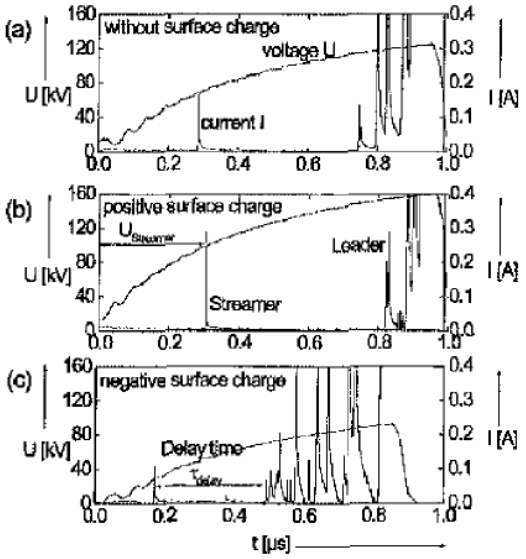


**Figure 1.** Instantaneous current and voltage during flashover at the surface of cylindrical epoxy insulator according to [9].

The creeping discharge propagation dynamics in $SF_6$ has been investigated by many researchers [7 – 11]. Okubo et al. [8] reported that the creeping discharge has the same dynamics as in air (Fig. 1). Tenbohlen and Schröder [9] analysed the surface discharge under lightning impulse (LI) voltage with different electrical charges deposition on the insulator surface. Figure 1 illustrates the current waveform from the inception to flashover with different electrical charges on the insulator surface. From figure 1, some similarities with discharge current propagating in air [13] can be noted; the current increases with the leader elongation until the discharge reaches the critical length. Then, the final jump occurs causing the full flashover.

Hayakawa et al. [7] analysed the mechanism of impulse creeping discharge propagation on charged PMMA (poly-methyl methacrylate) surface. Their results showed that the discharge propagation is influenced by the charged surface and can be explained by the streamer propagation and streamer-to-leader transition based on the precursor mechanism. On the other hand, according to Okubo et al. [8] and Beroual [3] and Beroual et al. [10, 11] the creeping discharge propagation depends on the specific capacitance of the solid insulator. The permittivity, the conductivity and the geometry of insulator affect the propagation of the surface discharge [10 - 12].

Peer-reviewed version available at Energies 2020, 13, 591; doi:10.3390/en13030591



Modelling and calculation of flashover voltage is not an easy task because the interaction of different parameters such as: gas pressure and its chemical constitution, physicochemical properties of the solid insulator, nature and distribution of the surface charges, etc. Different models enabling to compute the inception voltage of creeping discharges and flashover voltage of insulator in air at atmospheric pressure have been proposed [2, 3, 13]. Figure 2 depicts the different evolution steps of creeping discharge on insulator.

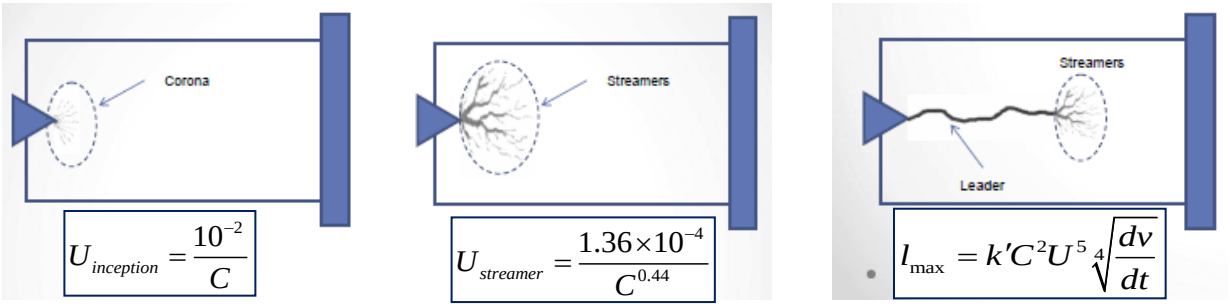


(a) (b) (c)

**Figure 2.** Steps of creeping discharges according to [2].

According to [2], the corona inception voltage depends on the equivalent capacitance of the system; it can be calculated with the following relationship [2]

$$U_{inception} = \frac{A}{C^a} \quad (1)$$

The second step is the appearance of streamers (figure 2-b). The streamers voltage inception is given by [2]

$$U_{streamer} = \frac{B}{C^b} \quad (2)$$

According to Toepler [3], the maximum (critical) length of the discharge that leads to flashover is

$$l_{max} = k \cdot C^2 \cdot U^5 \cdot \sqrt[4]{\frac{du}{dt}} \quad (3)$$

Then, if the voltage is increased, the discharge will be irreversible and propagates until flashover. In this case, the flashover voltage $U_{fov}$ can be calculated as well

$$U_{fov} = \frac{D}{C^d} \quad (4)$$

where

- C is the equivalent capacitance,
- A, B and D are parameters that depend on the geometry and the material of insulator, the kind of the discharge and the experimental conditions (gas, pressure, temperature, humidity, electrodes shape, voltage waveform…), respectively. Terms a, b and d are empirical parameters the values of which vary in the range 0.2 - 0.44.

These models involve only the capacitance of insulator and are mainly empirical.

Peer-reviewed version available at Energies 2020, 13, 591; doi:10.3390/en13030591



In the case of $SF_6$, Laghari [14] proposed a relationship of flashover voltage on the basis of the efficiency coefficient that represents the ratio of the flashover voltage for uniform electrical gradient distribution to the voltage breakdown of the same gap without insulator with the same configuration of insulator as well

$$V_{fov} = \frac{12.4}{\ln(V_b)} \cdot \frac{k_1}{k_2} \cdot \frac{\ln(\varepsilon_r)}{\varepsilon_r} \cdot V_b \quad (5)$$

$$\text{where } V_b = const + \left(\frac{E}{p}\right)_{cri} \cdot p \cdot d \quad (6)$$

$V_b$ is the breakdown voltage calculated according to Paschen law. $k_1$ and $k_2$ are parameters that depend on the roughness and the contact nature between the insulator and the electrodes. $\varepsilon_r$ is the permittivity of insulator.

Hama et al. [16] proposed a semi-empirical relationship of flashover voltage based on the mechanism leader/precursor:

$$V_{fov} = \frac{X_{Leader}}{D_{pol} V_{Leader}} + V_{Leader} \quad (8)$$

where $X_{Leader}$ and $V_{Leader}$ are the length and the voltage of the leader discharge, respectively; and $D_{pol}$ is a coefficient that dependent on the polarity of the applied voltage, the reduced critical electrical gradient and the shape of the electrodes, with

$$D_{pol} = const \times \left(\frac{E}{p}\right)_{cri} \times \phi\left(Ry_{\text{electrodes}}\right)$$

The application of this model shows results close to the experimental measurements but it is limited to the shape of the used insulators and the experimental conditions.

In the following, we recall the main principles of an analytical static model based on the electrical equivalent circuit and thermal discharge temperature we previously developed [1, 13].

## 3. Principal of circuit model

Surface discharges have similarities with spark (streamer/leader) discharges; i.e., a hot leader column and a streamers zone at its head [8, 9, 13, 17]. Based on Figure 3, the voltage along the discharge can be written as follows:

$$V_d = V_l + V_s = x_l E_l + x_s E_s = x_d\, r_d\, I \quad (9)$$

where $V_d$, $V_l$, $V_s$ are the voltages of the discharge, the leader channel and the streamers, respectively. $x_l$, $x_s$, $E_l$ and $E_s$ are respectively the length and the electrical gradient of the leader channel and the streamers. $x_d$, $r_d$, and I are resp. le discharge length, the discharge resistance and the current.

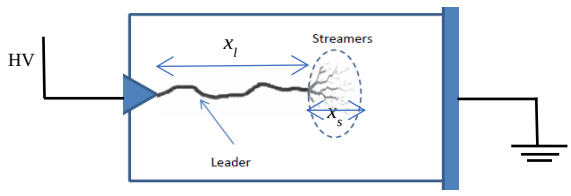


**Figure 3.** Illustration of leader column and streamers head of a discharge at the surface of an insulator.

Peer-reviewed version available at Energies 2020, 13, 591; doi:10.3390/en13030591



From Equation (9), we deduce the discharge resistance

$$r_d = \frac{x_l E_l + x_s E_s}{x_d I} \quad (10)$$

Where $x_d = x_s + x_l$

According to Equation (10), we can consider the creeping discharge as a non-linear resistance and assume that the discharge channel is a uniform cylinder.

Many researchers published photos of surface discharges indicating that there are two regions; the main luminous discharge (leader + streamer head) and less luminous branches, as illustrated in figures 4 and 5 [10, 18]. So, we can imagine that the presence of those less luminous discharges can be represented as a resistor parallel to the insulator surface. On the other hand, several researches investigations demonstrate the existence of a dark current in high pressurized gases that contribute to increase the insulator conductivity [19]. These currents contribute to the appearance of the second region (called luminous plasma) of depicted in figures 4 and 5.

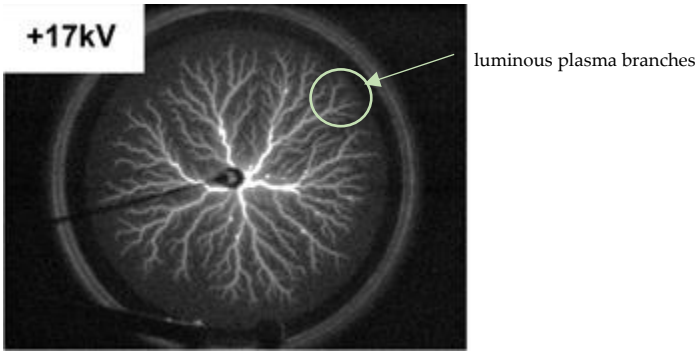


**Figure 4.** Surface discharge at the surface of insulator in SF6 with 3 bar under LI+ according to [10].

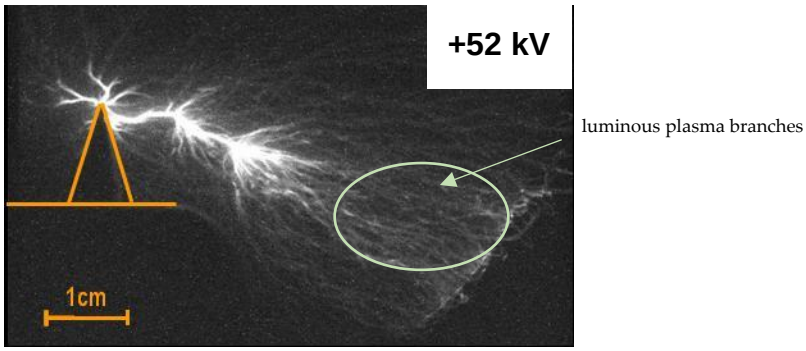


**Figure 5.** Surface discharge at the surface of coated electrode in SF6 with 1 bar under LI+ according to [18].

*3.1. Parameters of the circuit*

The model is based on an equivalent electrical circuit representing the electrical discharge, in series with the unbridged gap (the distance between the head of discharge and the opposite electrode) and consisting of a gas layer and of the solid dielectric at the interface (Figure 6). The gas layer is assumed to be equal to the diameter of the discharge channel. This model was developed elsewhere [13] in the case of air at atmospheric pressure and represent the instant when the discharge reaches a maximum length (called critical length) before the final jump [13]. In the following, we will adopt the

Peer-reviewed version available at Energies 2020, 13, 591; doi:10.3390/en13030591



same approach [13] with the assumption that the LI waveform can be considered as a quart-cycle of sine signal with a frequency about 0.3 MHz.

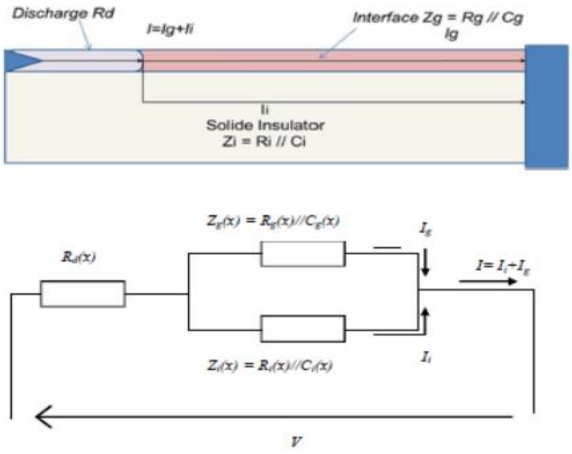


**Figure 6.** Insulator cylindrical model with a discharge channel and the corresponding equivalent electrical circuit.

The electrical Equation describing this circuit is

$$V = R_d(x)I + \left[Z_g(x) // Z_i(x)\right]I \tag{11}$$

Where

$$Z_g(X) = R_g(x) // C_g(x) = \frac{R_g(x)}{1 + j\omega R_g(x) C_g(x)} = \frac{r_g(L-x)}{1+\left(r_g c_g \omega\right)^2} - j\frac{r_g^2 c_g \omega (L-x)^2}{1+\left(r_g c_g \omega\right)^2}$$
$$Z_i(X) = R_i(x) // C_i(x) = \frac{R_i(x)}{1 + j\omega R_i(x) C_i(x)} = \frac{r_i(L-x)}{1+\left(r_i c_i \omega\right)^2} - j\frac{r_i^2 c_i \omega (L-x)^2}{1+\left(r_i c_i \omega\right)^2} \tag{12}$$

And

$$R_d(x) = r_d x = x\frac{\rho_d}{s_d} \quad ;$$

$$C_i(X) = \frac{c_i}{L-x} = \varepsilon_i \frac{s_i}{L-x} \; ; C_g(X) = \frac{c_g}{L-x} = \varepsilon_g \frac{s_g}{L-x} \; ; R_i(x) = r_i(L-x) = \rho_i \frac{L-x}{s_i} \; ; R_g(x) = r_g(L-x) = \rho_g \frac{L-x}{s_g}$$

$r_d$ is the linear resistance of the discharge channel; $r_i$, $r_g$, $c_i$, $c_g$, $\varepsilon_i$,, $\varepsilon_g$, $\rho_i$, and $\rho_g$, are respectively the linear resistance, capacitance, the permittivity and the resistivity, respectively of the solid insulator and the unbridged gap; $s_d$ is the cross section of the discharge channel, $s_i$ and $s_g$ are respectively the cross sections of the solid insulator and the layer of unbridged gap. $\omega$ is the pulsation ($\omega = 2\pi f$, $f$ being the frequency).

Then the equivalent impedance of the system will be

$$Z_{eq}(x) = r_d x + \frac{r_g r_i}{\alpha_g \alpha_i} G_1(L-x) + j\frac{r_g r_i}{\alpha_g \alpha_i} G_2(L-x) \tag{13}$$

where

$$\tau_g = \rho_g \varepsilon_g \omega = r_g c_g \omega$$
$$\tau_i = \rho_i \varepsilon_i \omega = r_i c_i \omega \tag{14}$$

Peer-reviewed version available at Energies 2020, 13, 591; doi:10.3390/en13030591



The product $\tau_i^2 >> 1$ and $\tau_g^2 >> 1$, then

$$\begin{cases} \alpha_i \approx \tau_i^2 \\ \alpha_g \approx \tau_g^2 \end{cases} \quad (15)$$

The terms $G_1$ and $G_2$ are

$$G_1 = \frac{z_1}{z_3 + z_4} \quad (16)$$

$$G_2 = \frac{z_2}{z_3 + z_4}$$

where

$$\begin{cases} z_1 = \left(\frac{r_g}{\tau_g^2} + \frac{r_i}{\tau_i^2}\right)\left(1 - \tau_g\tau_i\right) + \left(\frac{r_g}{\tau_g} + \frac{r_i}{\tau_i}\right)\left(\tau_g + \tau_i\right) \\ z_2 = \left(\frac{r_g}{\tau_g} + \frac{r_i}{\tau_i}\right)\left(1 - \tau_i\right) - \left(\frac{r_g}{\tau_g^2} - \frac{r_i}{\tau_i^2}\right)\left(\tau_g + \tau_i\right) \\ z_3 = \left(\frac{r_g}{\tau_g^2} + \frac{r_i}{\tau_i^2}\right)^2 \\ z_4 = \left(\frac{r_g}{\tau_g} + \frac{r_i}{\tau_i}\right)^2 \end{cases} \quad (17)$$

The square of the modulus of the equivalent impedance is

$$\left|Z_{eq}\right|^2 = \gamma x^2 + 2Lx\left[r_d\left(r_d - \frac{r_g r_i}{\tau_g^2\tau_i^2}G_1\right) - \gamma\right] \quad (18)$$

where

$$\gamma = \left(r_d - \frac{r_g r_i}{\tau_g^2\tau_i^2}G_1\right)^2 + \left(\frac{r_g r_i}{\tau_g^2\tau_i^2}G_2\right)^2 \quad (19)$$

According to Dhahbi *et al.* [20], the discharge propagates when the equivalent impedance decreases with increasing of its length. The discharge propagation condition is such as

$$\frac{d\left|Z_{eq}\right|^2}{dx} \le 0 \quad (20)$$

By differentiating Equation (18) with respect to x, we get

$$\frac{d\left|Z_{eq}\right|^2}{dx} = 2\gamma x + 2L\left[r_d\left(r_d - \frac{r_g r_i}{\tau_g^2\tau_i^2}G_1\right) - \gamma\right] \le 0 \quad (21)$$

Then

$$\frac{x}{L} - 1 \le \left[\frac{r_d}{\gamma\tau_g^2\tau_i^2}\left(r_g r_i G_1 - \tau_g^2\tau_i^2 r_d\right)\right] \quad (22)$$

Peer-reviewed version available at Energies 2020, 13, 591; doi:10.3390/en13030591



The total flashover of the solid dielectric is realized when Equation (22) is equal to zero, i.e., when the discharge length is equal to the total creeping (leakage) distance. This Equation can be considered as "the flashover condition". Therefore, the maximum length of the discharge corresponding to flashover or the discharge critical length is

$$x_{cri} = \frac{L}{\gamma\alpha_g\alpha_i}\left[\gamma\tau_g^2\tau_i^2 - r_d\left(r_d - \tau_g^2\tau_i^2 G_1\right)\right] = L\cdot n \tag{23}$$

where

$$n = \frac{1}{\gamma\tau_g^2\tau_i^2}\left[\gamma\tau_g^2\tau_i^2 - r_d\left(r_d - r_g r_i G_1\right)\right] \tag{24}$$

Where $0 < n < 1$

From Equation (12), we can derive the worst case that corresponding to

$$\frac{r_d}{\gamma\tau_g^2\tau_i^2}\left(r_g r_i G_1 - \tau_g^2\tau_i^2 r_d\right) \geq 0 \tag{25}$$

The term $\frac{r_d}{\gamma\tau_g^2\tau_i^2}$ is always positive, then

$$r_g r_i G_1 \geq \tau_g^2\tau_i^2 r_d \tag{26}$$

Equation (26) can be written as

$$\frac{\tau_g^2\tau_i^2}{G_1}\cdot\frac{r_d}{r_g r_i} = K \leq 1 \tag{27}$$

where

$$0 < K \leq 1 \tag{28}$$

Or

$$r_d \leq K\cdot G_1\cdot\frac{r_g r_i}{\tau_g^2\tau_i^2} \tag{29}$$

Condition (28) indicates that the discharge propagates when the ratio $K$ is between 0 and 1. This corresponds to the propagation condition in which the discharge length is sufficient for causing the final jump and thence the flashover [13].

On the other hand, the power loss per unit length $p_d$ in the discharge channel is

$$p_d = r_d I^2 \tag{30}$$

By combining Equations (30) and (26), it yields

$$I = \sqrt{\frac{p_d}{r_d}} \tag{31}$$

The square of the modulus of the voltage - Equation (11) is

Peer-reviewed version available at Energies 2020, 13, 591; doi:10.3390/en13030591



$$|V|^2 == |I|^2 \cdot |Z_{eq}|^2 \tag{32}$$

By substituting Equations (23), (24) and (30) in Equation (18), we get

$$|Z_{eq}|^2 = \beta L^2 \left( \frac{r_g r_i}{\tau_g^2 \tau_i^2} \right)^2 \tag{33}$$

with

$$\beta = K^2 G_1^{\,2} n^2 + \left( G_1^{\,2} + G_2^{\,2} \right) (1-n)^2 + 2K^2 G_1 n (1-n) \tag{34}$$

By substituting Equations (31) and (33) in Equation (32), we get the general relationship of flashover voltage

$$V_{FOV} = \frac{L}{\tau_g \tau_i} \sqrt{p_d \cdot \frac{r_g r_i}{r_d} \cdot \beta} \tag{34}$$

### *3.2. Thermal conductivity and discharge resistance*

According to the solution proposed by Frank-Kamenetski [21, 22], the energy dissipated by thermal conduction within the discharge channel is

$$P_d = 16\pi\lambda_d \frac{K_B}{W_i} T^2 \tag{35}$$

By combining (35) and (30), we get the final relationship of flashover voltage at atmospheric pressure

$$V_{FOV} = 4 \frac{L}{\tau_g \tau_i} T \sqrt{\frac{\pi K_B}{W_i} \cdot \lambda_d \cdot \frac{r_g r_i}{r_d} \cdot \beta} \tag{36}$$

In the case of air at atmospheric pressure, the thermal conductivity is calculated according to the following Equation [23]

$$\lambda(\theta) = \frac{\lambda_a}{1 + \frac{A_a (1 - v_a)}{v_a}} \tag{37}$$

where $\lambda_a$, $v_a$ and $A_a$ are the thermal conductivity, volume fraction and kinetic gas coefficient for air.

Also, the discharge resistance in air at atmospheric pressure is given by [24]

$$r_d(T) = r_{0d} \exp\left( W_i \Big/ 2K_B T \right) \tag{38}$$

where $r_{0d}$ is a constant in the range of operating temperatures of the discharge. $W_i$ represents the first ionization energy of the different species constituting the discharge channel; $K_B$ is the Boltzmann constant.

Peer-reviewed version available at Energies 2020, 13, 591; doi:10.3390/en13030591



In the case of $SF_6$, both discharge resistance and discharge thermal conductivity are function simultaneously of gas pressure and plasma temperature [25, 26].

$$\lambda_d = \Gamma(T, p)$$
$$\sigma_d = \Sigma(T, p) \quad (39)$$

According to Pinnekamp and Niemeyer [27], and Niemeyer et al. [28], the temperature of the leader discharge is between 2400 K and 2800 K. On the other hand, on the basis of the transport parameters data of $SF_6$ published in the literature [25, 26], we plot the thermal conductivity as function of gas pressure (Figure 10) and the discharge resistance against gas pressure (Figure 11) for a range of temperature between 2500 K and 3500 K. From these figures, we can derive numerical empirical formulae of the discharge thermal conductivity and discharge resistance against pressure for a given temperature:

$$\sigma_d = A.p^{-m} \quad (40)$$

$$\lambda_d = a_0 + \ldots + a_n p^n \quad (41)$$

where p is the gas pressure; a and A are empirical parameters.

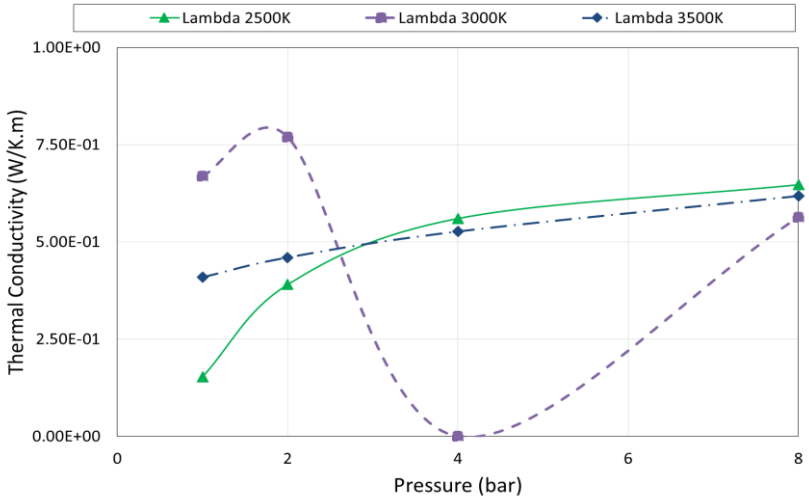


**Figure 7.** Discharge thermal conductance of discharge vs. variation with pressure with for different temperatures.

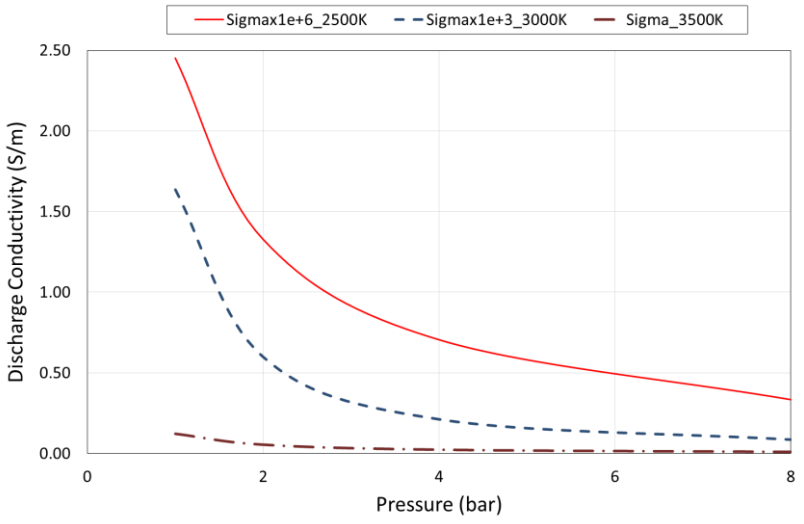


**Figure 8.** Discharge resistance variation with vs. pressure with different temperatures at 2500 and 3000 K, respectively.

Peer-reviewed version available at Energies 2020, 13, 591; doi:10.3390/en13030591



## 4. Application

To validate the proposed model, we first calculate the flashover voltage of cylindrical epoxy insulators in air at atmospheric pressure. The second application will be for the same kind of insulator in $SF_6$ gas medium. The computed flashover voltages are compared with the experimental data reported by other researchers as in [12, 13, 15, 29]. Table 1 gives the characteristics of the used insulator in the computations.

| Insulator | Material | Diameter | Length | Reference | Gas | Pressure |
|---|---|---|---|---|---|---|
| 1 | Epoxy | 25 | 70 | [13] | Air | Atmospheric |
| 2 | Epoxy | 25 | 60 | [12] | $SF_6$ | Variable |
| 3 | Epoxy | 25 | 45 | [29] | $SF_6$ | Variable |
| 4 | Epoxy | 30 | 10 | [15] | $SF_6$ | Variable |

**Table 1.** Characteristics of used insulators from literature used in modelling.

The lightning impulse voltage frequency is calculated based on the following Equation [30]

$$f = 0.35 / T_R \quad (42)$$

$T_R$ is the rising time of the voltage front equal to 1.2 μs.

### 4.1 *Air at normal atmospheric conditions*

Figures 9 illustrates the results of the application of the proposed model in air at atmospheric pressure. We compare our model with the experimental data of [13], a model we developed earlier [1] and Toepler's model. The temperature of discharge was taken between 1800 K and 2000 K which corresponds to a leader phase on insulator surface. The resistance of air ranges from $10^{23}$ to $10^{25}$ Ω/cm; its dielectric constant being equal to 1. The effect of humidity is neglected.

By comparing flashover voltage given by Equation (36) and the other models, we observe that the impedance of the interface between the head of the discharge and the opposite electrode plays an important role (Figure 9). It modulates the breakdown process before the final jump of the discharge (flashover) as described in [12].

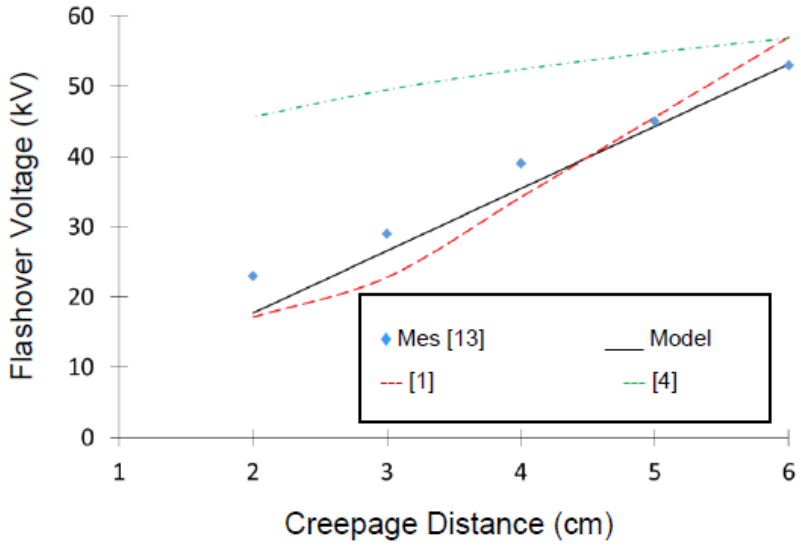


**Figure 9.** Comparison between calculated and measured flashover voltage vs. creepage distance in air at atmospheric pressure for insulator 1.

Peer-reviewed version available at Energies 2020, 13, 591; doi:10.3390/en13030591



### 4.2 $SF_6$ at variable pressure

In the case of $SF_6$, we use Equations (37), (40) and (41) to compute the flashover voltage and its dependency on the gas pressure and temperature. The temperature of the discharge was taken between 2500 K and 3500 K.

A specific consideration for the resistance of the gas at the interface is required in the case of pressurised $SF_6$. In fact, experimental results concerning flashover of solid insulators on pressurised gases suggest that the discharge tends to stick to the insulator surface when the gas pressure increases [8], [12]. On the other hand, according to Figures 4 and 5, the gap between the discharges head and the ground electrode appears like an ionized cylinder. Knowing also that the attachment of the pressurised gas increases with pressure, we infer that the resistance of the interface between the discharge head and the grounding electrode depends on the gas pressure also.

On the basis of the data reported in the literature [25, 26], we assume that the resistance of the interface can be represented as a cylindrical plasma with a temperature between 1000 K and 1500K. In this range of temperature, the plasma resistivity increases with the gas pressure as depicted in figure 10. As can be observed in this figure, the assumption of a plasma with a temperature varying between 1200 K and 1400 K is a good approximation since the resistivity is increasing with pressure for all temperatures. The dielectric constant being equal to 1 and the effects of surface charge accumulation and humidity are not considered.

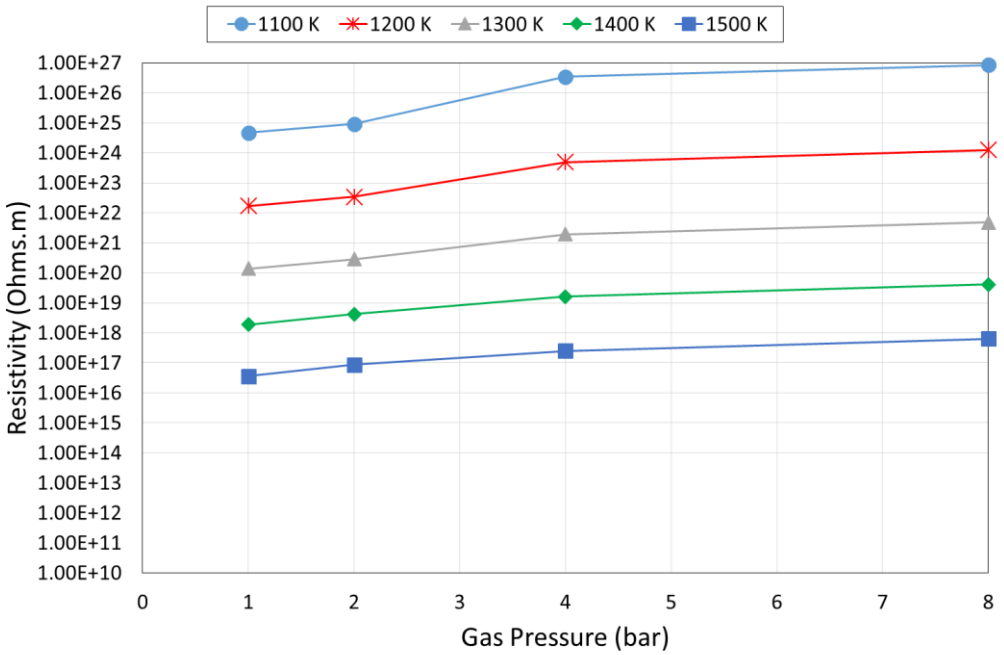


**Figure 10.** Resistivity of the $SF_6$ plasma at non thermal regime vs gas pressure et different temperatures.

Figure 11 illustrates the comparison of the calculated flashover voltage with the data of Slama et al. [12] for insulator 2 of table 1. It can be seen that the calculated flashover voltages are close to the measured values indicating that flashover voltage tends to be stable with the pressure increase.

Peer-reviewed version available at Energies 2020, 13, 591; doi:10.3390/en13030591



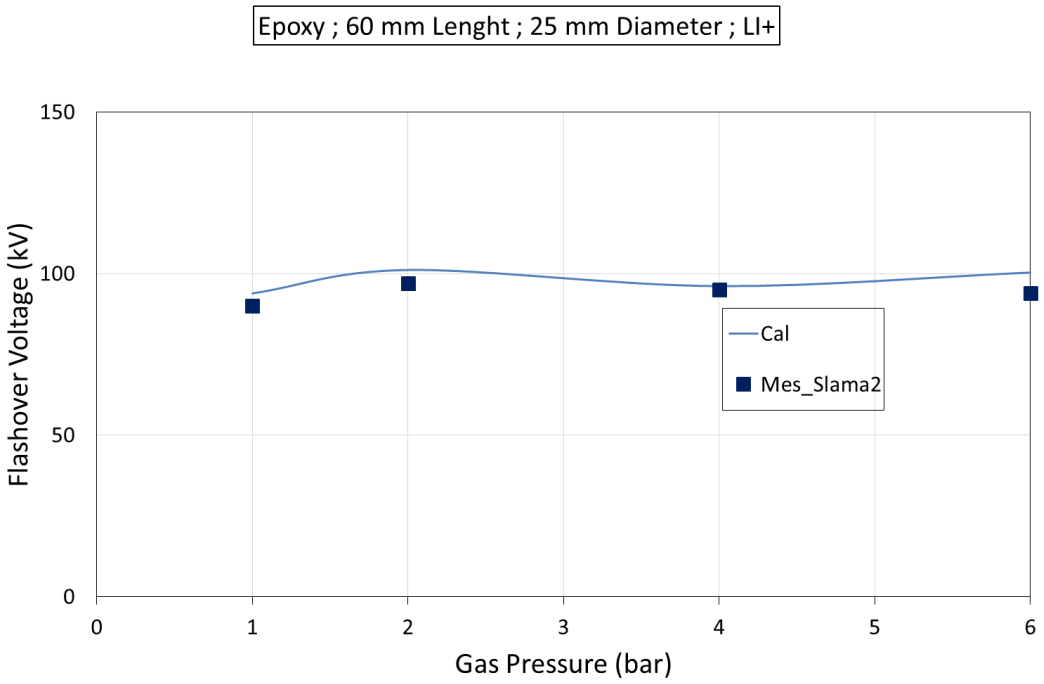


**Figure 11.** Comparison between calculated and measured flashover voltage vs. gas pressure for insulator 2 with 60 mm length and 25 mm diameter.

In Figure 12, we compare the calculated flashover voltage with the data of [29] obtained with insulator 3. In this work, Moukengué and Feser [29] present results of flashover voltages as function of gas pressure for different tests: one for a single impulse shot and the second for five impulse shots. We note that the calculated flashover voltage are close to the experimental measured values.

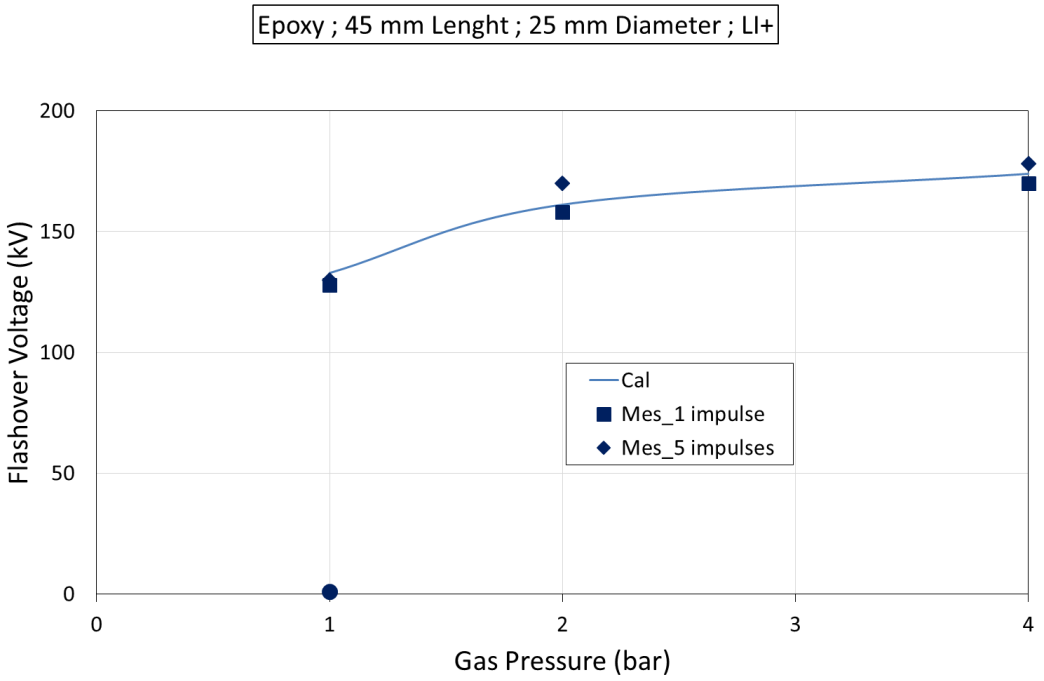


**Figure 12.** Comparison between calculated and measured flashover voltage vs. gas pressure for a cylindrical epoxy insulator 4 with 45 mm length and 25 mm diameter.

Peer-reviewed version available at Energies 2020, 13, 591; doi:10.3390/en13030591



Figure 13 shows the comparison of the results using the developed model and the data of [15] with insulator 4. Again, we observe that the calculated flashover voltages are close to the experimental ones.

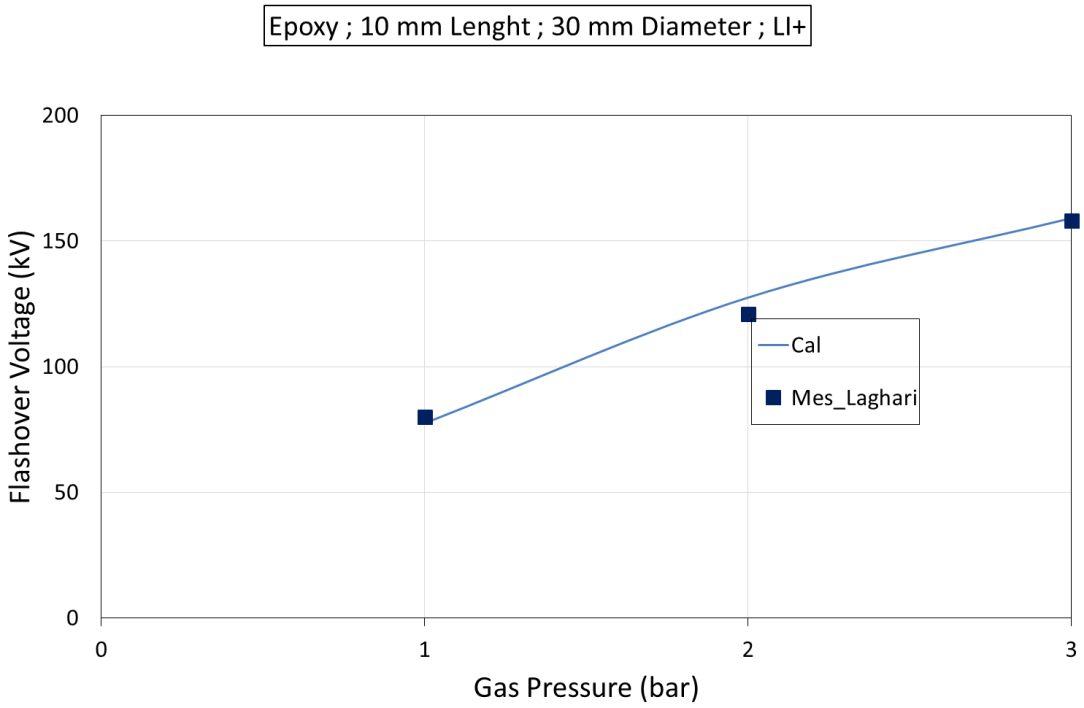


**Figure 13.** Comparison between calculated and measured flashover voltage vs. gas pressure for a cylindrical epoxy insulator with 10 mm length and 30 mm diameter.

## 5. Conclusions

In this paper, a model is developed for surface discharges and flashover voltage modelling in air at atmospheric pressure and compressed $SF_6$. The proposed analytical model based on the equivalent electrical circuit representing the discharge along the insulator surface and the thermal properties of the discharge. The model was first applied for air at atmospheric pressure in order to validate it against established models and data. The obtained results are very close to the measured values. In the case of $SF_6$, it is assumed that the area between the discharge head and the ground electrode can be considered as a cylindrical plasma. The application of this model to various configurations taken from literature shows that the calculated flashover voltage magnitudes are close to the measured values and exhibit similar trend. The proposed model can be a first step to develop a tool for the prediction and the design of the solid insulation in GIS and GIL filled with $SF_6$.

**Author Contributions:** "conceptualization, M.E.A.S, A.B. and A.M.H; methodology, M.E.A.S, A.B. and A.M.H; validation, M.E.A.S, A.B. and A.M.H.; formal analysis, M.E.A.S, A.B. and A.M.H.; investigation, , M.E.A.S.; writing—original draft preparation, , M.E.A.S.; writing—review and editing, , M.E.A.S, A.B. and A.M.H.; visualization, , M.E.A.S, A.B. and A.M.H.

**Acknowledgments:** Authors would thank Mrs Sylvain Nichele, Alain Girodet and Paul Vinson form SuperGrid Institute (France) for their help.

**Conflicts of Interest:** The authors declare no conflict of interest.

Peer-reviewed version available at Energies 2020, 13, 591; doi:10.3390/en13030591



## References


1. M. El-A. Slama, A. Beroual, A. Girodet and P. Vinson, "Characterization and Mathematical Modelling of Surface Solid Insulator in Air", International Symposium on High Voltage Engineering, August 24-28, Plzen, Czech Republic, 2015.
2. Al-Arainy, A. Beroual and N. Malik, "Experiments in High Voltage Engineering" King Saud University, Academic Publishing and Press, 2014.
3. A. Beroual, "Creeping Discharges at Liquid/solid and Gas/Solid Interfaces: Analogies and Involving Mechanisms" IEEE 20th International Conference on Dielectric Liquids (ICDL), Roma, Italy, June 23-27, 2019.
4. M. Toepler, "Über die physikalischen Grundgesetze der in der Isolatorentechnik auftretenden elektrischen Gleiterscheinungen" Archiv für Elektrotechnik, Nr. 10, S. 157-185, 1921.
5. Alan H. Cookson ".Review of high-voltage gas breakdown and insulators in compressed gas", IEE PROC, Vol. 128, Pt. A, No. 4, pp 303-312, May 1981.
6. T. S. Sudarshan and R. Dougal, "Mechanisms of surface flashover along solid dielectrics in compressed gases", Review, IEEE Trans. Electr. Insul., No. 21, pp. 727-746,1986.
7. N. Hayakawa, Y. Ishida, H. Nishiguchi, M. Hikita and H. Okubo, "Mechanism of impulse creepage discharge propagation on charged dielectric surface in SF6 gas", T. IEE Japan, Vol. 116-B, No. 5, 1996, pp 600-606.
8. H Okubo, M. Kanegami, M. Hikita and Y. Kito,"Creepage Discharge Propagation in Air and SF6 Gas Influenced by Surface Charge on Solid Dielectrics", IEEE Transactions on Dielectrics and Electrical Insulation Vol. 1 No. 2, pp. 204- 304, 2004.
9. S. Tenbohlen and G. Schröder, Discharge Development over Surfaces in SF6, IEEE Trans on DEI, Vol.7, n°2, pp. 241-246, April 2000.
10. A. Beroual, M-L. Coulibaly, O. Aitken, A. Girodet, Investigation on creeping discharges propagating over epoxy resin and glass insulators in presence of different gases and mixtures, Eur. Phys. J., Appl. Phys., 2011, 56, (03), pp. 30802 –30809
11. A. Beroual, M-L. Coulibaly, O. Aitken, A. Girodet, Effect of micro-fillers in PTFE insulators on the characteristics of surface discharges in presence of SF6, CO2 and SF6 –CO2 mixture, IET Gener. Transm. Distrib., 2012, 6, (10), pp. 951 –957.
12. M. El-A. Slama, A. Beroual, A. Girodet and P. Vinson, "Barrier effect on Surface Breakdown of Epoxy Solid Dielectric in SF6 with Various Pressures", Conference on Electrical Insulation and Dielectrics Phenomena, Toronto, Canada, Oct 2016, CEIDP 2016.
13. M. El-A. Slama, A. Beroual, A. Girodet and P. Vinson, "Creeping Discharge and Flashover of Solid Dielectric in Air at Atmospheric Pressure: Experiment and Modelling", IEEE Transactions on Dielectrics and Electrical Insulation, 23 (5), pp.2949 – 2956, 2016.
14. M. A. Douar, A. Beroual and X. Souche "Creeping discharges features propagating in air at atmospheric pressure on various materials under positive lightning impulse voltage – part 2: modelling and computation of discharges' parameters" IET Gener. Transm. Distrib., 2018, 6, (12), pp. 1429-1437.
15. R. Laghari " Spacer Flashover in Compressed Gases ", in IEEE Trans. On EI Vol. EI-20 n°1, Feb 1985.
16. H. Hama et al. «Estimation of Breakdown Voltage of Surface Flashover Initiated from Triple Junction in SF6 Gas", In EEJ, Vol. 116, n°5, 1996.
17. R. T. Waters, A. Haddad, H. Griffiths, N. Harid and P. Sarkar, "Partial-arc and Spark Models of the Flashover of Lightly Polluted Insulators", IEEE Transactions on Dielectrics and Electrical Insulation, Vol. 17, No. 2, pp. 417-424, April 2010.
18. J. E. M. Kessler "Isoliervermögen hybrider Isoliersysteme in gasisolierten metallgekapselten Schaltanlagen (GIS)", PhD Thesis, Technische Universität München, Germany, 2011.
19. L. Zavattoni "Conduction phenomena through gas and insulating solids in HVDC Gas Insulated Substations, and consequences on electric field distribution", PhD Thesis, University of Grenoble, france, 2014.

Peer-reviewed version available at Energies 2020, 13, 591; doi:10.3390/en13030591




20. N. Dhahbi-Megriche, A. Beroual and L. Krähenbühl, "A New Proposal Model for Polluted Insulators Flashover", J. Phys. D. Appl. Phys., Vol. 30, N°5, pp. 889-894, 1997.
21. A. Fridman et al, "Gliding arc discharge", Progress in Energy Combustion Science 25, 1999, Elsevier Sciences Ltd, pp 211-231.
22. A. Fridman, "Plasma chemistry", Cambridge University Press, 2008.
23. [17] W. McElhannon and E. McLaughlim, "Thermal Conductivity of Simple Dense Fluid Mixtures", Proceeding of the Fourteenth International Conference on Thermal Conductivity, Edited by P. G. Klemens and T. K. Clen, 1975.
24. M. El-A. Slama, A. Beroual and H. Hadi, "Analytical Computation of Discharge Characteristic Constants and Critical Parameters of Flashover of Polluted Insulators", IEEE Trans. Dielectr. Electr. Insul., Vol. 17, No. 6; pp. 1764-1771, 2010.
25. Linlin Zhong, Mingzhe Rong, Xiaohua Wang, Junhui Wu, Guiquan Han, Guohui Han, Yanhui Lu, Aijun Yang, and Yi Wu, "Compositions, thermodynamic properties, and transport coefficients of high temperature $C_5F_{10}O$ mixed with $CO_2$ and $O_2$ as substitutes for $SF_6$ to reduce global warming potential", AIP Advances 7, 075003 (2017).
26. M. J. Assael, I. A. Koini, K. D. Antoniadis, M. L. Huber, I. M. Abdulagatov, and R. A. Perkins, "Reference Correlation of the Thermal Conductivity of Sulfur Hexafluoride from the Triple Point to 1000 K and up to 150 MPa", Journal of Physical and Chemical Reference Data 41, 023104 (2012).
27. L. Niemeyer and F. Pinnekamp, "Leader discharges in SF6", Journal of Physics D: Applied Physics, Vol. 16, 1983, pp 1031-1045.
28. N. Wiegart, L. Niemeyer, F. Pinnekamp, W. Boeck, J. Kindersberger, R. Morrow, W. Zaengl, M. Zwicky, I. Gallimberti and S. A. Boggs, "Inhomogeneous Field Breakdown in GIS — The Prediction of Breakdown Probabilities and Voltages: Parts I, II, and III", IEEE Transactions on Power Delivery, Vol. 3, No. 3, pp. 923-946, July 1988.
29. A. Moukengué lmano and K. Feser, "Flashover behavior of conducting particle on the spacer surface in compressed $N_2$, 90%$N_2$+10%$SF_6$ and $SF_6$ under lightning impulse stress", International Symposium on Electrical Insulation (ISEI 2000), Anaheim, USA, April 2000.
30. M. Ianovici et J-J. Morf, "Compatibilité électromagnétique", Presses Polytechniques et Universitaires Romandes, Lausanne, Suisse, 1979.